Over-Current Protection Scheme for SiC Power MOSFET DC Circuit Breaker

Yuan Zhang, *Student Member,IEEE* and Yung C. Liang*, *Senior Member,IEEE*
Department of Electrical and Computer Engineering, National University of Singapore, Singapore
*Contact Author E-mail: chii@nus.edu.sg

***Abstract*—The electronic circuit breaker used in DC microgrids are required to work within their safe operating areas bounded by temperature, voltage and current limits. Traditional approach managed to protect these switches through rapid current cut-off operations at over-load or fault situations, but failing to avoid the disturbance induced by transient current surges or noises which are not harmful to the grid operations. Aiming to increase the quality of circuit breaker operations and furthermore improve its reliability, this paper proposed a SiC MOSFET based DC circuit breaker based on the variable time-delay protection scheme. The cut-off operations only take place after proper delay time, which are precisely catered according to the transient thermal properties of SiC devices and the properties of DC loads. The proposed scheme has been implemented with hardware prototype and experimentally verified under different fault situations.**

I. INTRODUCTION

DC microgrids are used in modern buildings, vessels and vehicles as efficient delivery interconnects between DC energy sources and loads. Similar to AC grids, circuit breakers in DC microgrids carry the function on grid protection. Therefore, these breakers not only do endure grid normal operations and but also be capable of cutting off currents under various fault levels. Solid-state DC circuit breakers made of the modern wide bandgap power semiconductor devices, such as silicon carbide (SiC) and gallium nitride (GaN) MOSFETs can largely enhance the switching performance much better than the mechanical counterparts [1,2]. These wide bandgap power devices have higher voltage sustainability, higher temperature tolerance and faster switching speed with simple driving requirements [3]. For the voltage level of 400V for the DC microgrids, the use of SiC power devices is a prominent choice for the circuit breaker due to their remarkable performance merits [4,5].

Besides protecting loads, electronic circuit breakers also need to protect themselves from large fault current. The possible risks faced are in two conditions. In moderate fault situation, the breaker may suffer from thermal stress caused by joint overheating [6] if the fault current is not cleared in time. In serious conditions like short-circuit faults, the electromagnetic force induced by large fault current cracks the bond wires of electronic switches and causes physical damage to the semiconductor dies[7].

Several schemes had been proposed to protect SiC devices from thermal and mechanical damage [8-10]. In [8], it came out with a method to collect temperature information by thermal coupler in order to prevent the SiC devices from overheating damage. However, the use of thermal coupler is not welcomed since it increases the cost and complexity of the control circuit. Some achieved rapid fault isolation function for SiC devices based on technique of micro-controllers [9]. The fault current can be interrupted within a few micro-seconds. Such a rapid interruption scheme may result in premature current interrupt on transient surge or noise. In practice, in moderate fault situations with relatively low fault current level, SiC devices will not be burned out immediately until a few milliseconds later. This indicates that smaller fault current can be cut off after an allowable delay time, in order to avoid the false alarm on current surge or noise.

In this paper, a solid-state circuit breaker based on SiC power MOSFET with variable time-delayed protection scheme for DC microgrids is developed. The turn-off delay time varies according to the transient thermal property of the SiC power MOSFET device, as well as the load protection delay time according to user's preset requirements. The introduction of variable delay time ensures the circuit breaker function with high reliability under various overcurrent transient situations.

II. VARIABLE TUNR-OFF DELAY TIMES FOR PROTECTION

A. Three Different Fault Conditions

Large current caused by overloading or faults in DC microgrids will need to be interrupted and isolated in order to preserve the grid integrity. If fault current I_D exceeds the load current limitation I_{LD}, load may suffer and break down. If I_D

978-1-4799-5776-7/14/$31.00 ©2014 IEEE

exceeds the continuous current rating I_{OC} of semiconductor switch, the switch will suffer thermal stress and damage. If I_D exceeds the pulsed current rating I_{SC}, electromagnetic damage might happen to the semiconductor switch [7].

Three different fault levels showed in Fig. 1 are protected in DC microgrid. The corresponding protection operations in these three fault situations have different assigned turn-off delay time as shown in Fig. 2.

(1) Overload fault ($I_{LD} \le I_D < I_{OC}$): As shown in Fig. 1(a), fault current I_D should be interrupted with the allowable turn-off delay time to ensure the safety of DC load. Both load current limitation I_{LD} and turn-off delay time are adjustable according to the load protection requirement. Usually, delay time varies from a few milliseconds to a few seconds for different DC load types [11].

(2) Large overcurrent fault ($I_{OC} \le I_D < I_{SC}$): Switch is short circuited through the impedance Z_f [12] as in Fig. 1(b). Protection operation is required within the Safe Operation Area (SOA) thermal limit to avoid overheating. As shown in Fig. 2, the allowable delay time varies exponentially with the overcurrent magnitude I_D according to the transient thermal property of the semiconductor switch in the ranges of milliseconds.

(3) Short-circuit fault ($I_D \ge I_{SC}$): This is the most serious situation with almost zero fault impedance shown in Fig. 1(c). Fault current I_D should be cut off as soon as possible to avoid electromagnetic force damage to the power semiconductor devices. The maximum turn-off delay time is usually in microsecond for rapid operation.

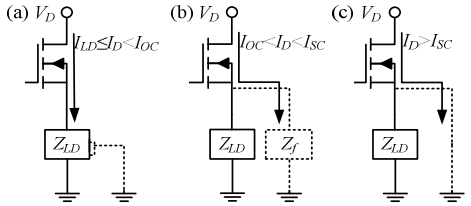

Figure 1. Three fault types in DC microgrids (a) oveload fault (b) large overcurrent fault (c) short-circuit fault

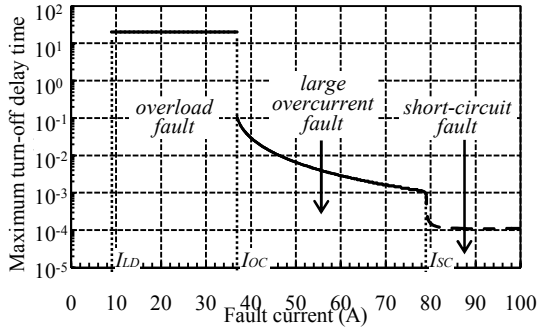

Figure 2. The variable time-delay protection scheme for DC mcrogrid by SiC power MOSFET switch CMF20120D

B. Trasient Thermal Response of SiC Switch

At large fault current, SiC device is heated with temperature gradually rising on thermal capacitance [10]. The transient thermal response of SiC MOSFET can be derived based on the equivalent thermal circuit shown in Fig. 3(a), in which thermal capacitance and resistance are modelled by electric capacitor and resistor. The resistance R_{JC} and capacitance C_{JC} between junction and case, and resistance R_{CA} and capacitance C_{CA} between case and ambient are used in the circuit model. Temperatures of junction, case and ambient are equivalent by node voltages assigned as T_J, T_C and T_A respectively. Power dissipation by semiconductor junction is equivalent to a current source signed as P_D. Transient thermal response can be treated as the process that temperature T_J varying with power P_D. Normally, the time constant $\tau_{CA}=R_{CA}C_{CA}$ is a few seconds if a heatsink is used, which is much larger than the time scale of transient thermal response considered in this paper. Thus it is reasonable to ignore the effects of R_{CA} and C_{CA}, and analyze the simplified model in Fig. 3(b) with constant case temperature T_C.

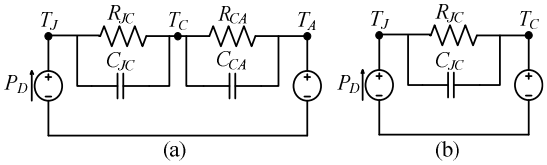

Figure 3. Equivalent model for transient thremal response of SiC MOSFET (a) Detailed model (b) Simplifed model

In Fig. 3(b), junction temperature T_J increases according to

$$T_J(t) = P_D Z_{JC}(t) + T_C \tag{1}$$

where Z_{JC} is the transient thermal impedance related to R_{JC} and C_{JC}; T_C is a constant value depending on the initial operating condition as

$$T_C = P_{D0} R_{CA} + T_A \tag{2}$$

where P_{D0} is the initial dissipation power; R_{CA} is the case-to-ambient thermal resistor; T_A is the ambient temperature.

In (1), the value of power dissipation P_D depends on the on-state resistance R_{DS} and drain current I_D as

$$P_D = I_D^2 R_{DS} \tag{3}$$

where R_{DS} changes with I_{DS} according to

$$R_{DS} = R_{DS0} + 0.001(I_D - 20) \tag{4}$$

R_{DS0} in (4) is temperature-dependent and is at I_D=20A. Its value is described in the datasheet of SiC MOSFET [13] as following

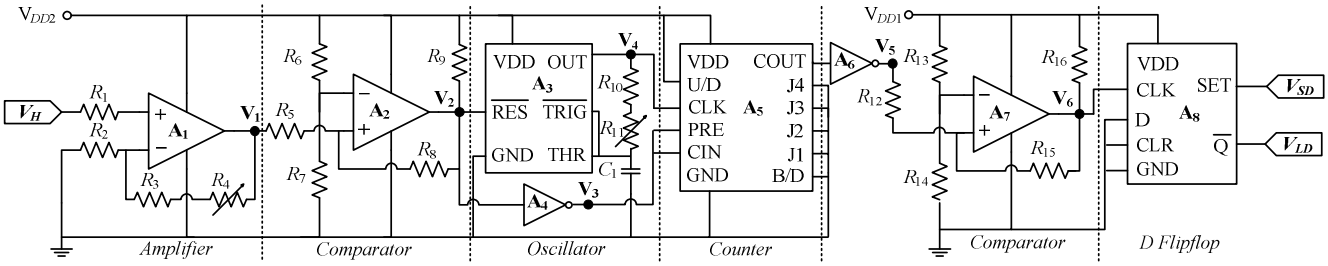

Figure 4. Protection circuit for DC load

$$R_{DS0} = \begin{cases} 0.087 & 25℃ \le T_J \le 63℃ \\ 0.087\left[a_1 {T_J}^2 - a_2 T_J + a_3\right] & T_J > 63℃ \end{cases} \quad (5)$$

where coefficients a_1, a_2 and a_3 are 0.00006, 0.0044 and 1.04.

Z_{JC} in (1) can also be obtained from datasheet as

$$Z_{JC} = \begin{cases} 10^{-b_1 c^3 - b_2 c^2 - b_3 c - b_4} & 10^{-6} s < t < 0.14 s \\ 0.53 & t \ge 0.14 s \end{cases} \quad (6)$$

where coefficients b_1, b_2, b_3 and b_4 are 0.01, 0.20, 0.38 and 0.40; c is the common logarithm of duration t with fault current.

Based on (1)-(6), the allowable time for SiC MOSFET to exceed its maximum junction temperature rating can be derived using numerical iteration method and obtained as depicted in Fig. 2. This delay-time value is treated as the maximum turn-off delay time on overcurrent fault, within then the fault current has to be interrupted [14]. Here the maximum junction temperature is set to be 200ºC to maintain thermal reliability [15], and pulsed current rating I_{SC} is set at 78A according to the datasheet [13].

III. Proposed Circuit for Time-Delayed Protection

Since the allowable turn-off delay time of three fault types are in different time scale, the proposed circuit is designed for load protection and device protection respectively.

A. Load Protection Circuit

Fig.4 shows the protection circuit for DC load. The input signal V_H comes from the hall-effect sensor which senses drain current I_D of MOSFET with proportional voltage signal output according to

$$V_H = V_{H0} + k_S I_D \quad (5)$$

where V_{H0} is the quiescent output voltage of hall-effect sensor when I_D equals to zero; k_S is the sensitivity of the sensor. In this paper, hall-effect sensor with V_{H0}=0.6V, k_S=0.04V/A is used.

Under overload situation with I_D exceeding load rating I_{LD}, V_H increases accordingly and makes the output signal V_1 of comparator jump to a high level. In this situation, the delay time circuit formed by oscillator and counter starts to operate, and produces a positive pulse V_5 which induces a positive edge V_{LD}.

As mentioned before, the current threshold I_{LD} and turn-off delay time t_d for overload depend on the requirement of the DC load and thus should be adjustable by users. This can be achieved by changing the value of resistance R_4 and R_{11}. I_{LD} varies its value with R_4 according to

$$I_{LD} = \left[\frac{V_{th1}}{1+(R_3+R_4)/R_2} - V_{H0}\right]\frac{1}{k_s} \quad (6)$$

where V_{H0} and k_S are current sensor's coefficients shown in (5); V_{th1} is the threshold of comparator set by A_2 in Fig.4.

Turn-off delay time t_d then varies with resistance R_{11} according to

$$t_d = 20(R_{10} + R_{11})C_1 \quad (7)$$

B. Protection Circuit for SiC MOSFET Switches

Fig. 5 shows the protection circuit for SiC switching device. When overcurrent fault happens, fault current I_D exceeds the current threshold I_{OC}. V_H surges and makes the output voltage V_7 increase. V_7 gradually charges capacitor C_2 in the time delay circuit. Once voltage V_8 of C_2 exceeds the threshold value V_{th2} of comparator A_{10} after delay time t_d, a positive edge V_{OC} is produced.

The threshold I_{OC} of switch protection is set based on

$$I_{OC} = [V_{th2}R_{18}/(R_{18} + R_{19}) - V_{H0}]/k_S \quad (8)$$

and the delay time t_d corresponding to fault current level I_D can be represented as

$$t_d = -\tau\, ln\left[1 - \frac{V_{th2} - (1+R_{19}/R_{18})\, R_{21} V_{H0}/(R_{20}+R_{21})}{(1+R_{19}/R_{18})\, R_{21}(V_{H0}+k_S I_D)/(R_{20}+R_{21})}\right] \quad (9)$$

where τ is the time constant for RC circuit. In overcurrent fault with relatively small I_D, V_7 is small so that zener diode Z_1 does not break down. Thus τ is larger and can be

estimated as $\tau = R_{OC}C_1$, where R_{OC} is the parallel resistance of R_{20} and R_{21}. In short-circuit situation with larger I_D, τ decreases to $R_{SC}C_1$ due to the breakdown of Z_1. Here R_{SC} is the parallel resistance of R_{OC} and the dynamic resistance of Z_1. The decease of τ meets the rapid turn-off action required in short-circuit fault.

C. Control of Gate Driving Circuit

Fig. 6 shows the continuously-on gate driver of the SiC MOSFET high-side switch [16]. As can be seen, the driver is controlled by three signals: V_{LD} from load protection circuit, V_{OC} from switch protection circuit, and manual command V_{SD}. At the initial stage, a positive pulse V_{SD} is required to turn on the SiC MOSFET. Once fault happens, positive pulse V_{OC} or V_{LD} is produced after allowable delay time and SiC switch is turned off.

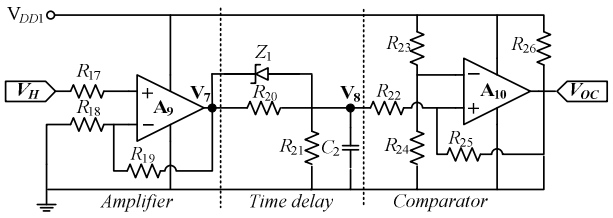

Figure 5. Protection circuit for SiC MOSFET switch

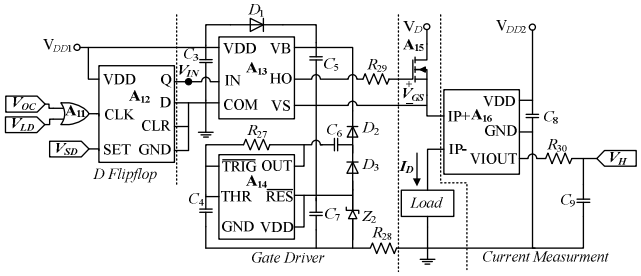

Figure 6. High-side drive and current sensor for SiC MOSFET Switch

IV. Experimental Verification

To verify the function of time-delayed protection circuit developed in Fig. 4 to Fig. 6, the experimental measurements were taken. The component values in the designed circuits are listed as follows:

R_1, R_2, R_3, R_{10}, R_{17}, R_{18}=1kΩ, R_6=3.3kΩ, R_{15}=47kΩ,

R_5, R_9, R_{12}, R_{16}, R_{24}, R_{26}=2.2kΩ, R_7, R_{13}=4.7kΩ,

R_8, R_{25}=33kΩ, R_{19}=2.7kΩ, R_{14}, R_{22}=1.5kΩ, R_{23}=10kΩ

R_{20}, R_{21}=15kΩ, R_{28}=1MΩ, R_{29}=560Ω, R_{30}=120Ω;

R_4=0~5kΩ, R_{11}=0~1MΩ;

C_1, C_3, C_4=1μF, C_2=0.33μF, C_6=10nF,

C_5, C_7, C_8=0.1μF, C_9=0.033μF;

D_1, D_2, D_3: 1N4002;

Z_1: BZX85C11, Z_2: BZX85C15;

A_1, A_2, A_7, A_9, A_{10}: LM392, A_3, A_{14}: ICM7555,

A_4, A_6: CD4049, A_5: CD4029, A_8, A_{12}: CD4013,

A_{11}: CD4075, A_{13}: IR2117, A_{15}: CMF20120D;

V_{DD1}: 15V, V_{DD2}: 5V.

A. Load Protection Test

In the load protection test, resistance R_4 and R_{11} are set to be 2.7kΩ and 140kΩ respectively. According to (6) and (7), the current threshold I_{LD} for load protection is 3.4A, while turn-off delay time is about 2.8s. Since the supply DC voltage V_D in Fig. 6 is 400V, the resistance of DC load is set to be 54Ω in order to create the overload fault. Measured waveforms on load protection are shown in Fig. 7. As seen, the SiC MOSFET is turned on at 0.72s when gate voltage V_{GS} raises to 15V under the function of positive pulse V_{SD} in Fig. 6. Current I_D surges to 9.6A and sets at 5.4A exceeding the threshold current level I_{LD}. The turn-off command V_{LD} is produced after 2.78s and fault current I_D is cut off at 3.5s.

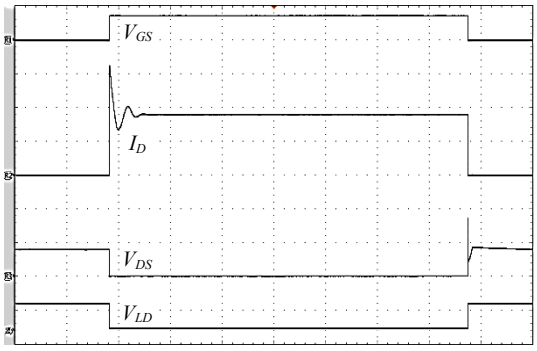

Figure 7. Tested waveform of load protection circuit. V_{GS}: 20V/div, I_D: 3A/div, V_{DS}: 500V/div, V_{LD}: 20V/div, *time*: 0.4s/div

The relationship between current threshold I_{LD} and resistance R_4 is verified and showed in Fig. 8, in which solid line is the calculated outcome based on (6) and dots are the measured data. The relationship between turn-off delay time and resistance R_{11} is showed in Fig. 9. Both figures verify that the measured data match the prediction closely, which indicates that proposed protection circuit can be adjusted according to different load requirements.

B. Switch Protection Test

In this test, protection circuit is required to respond to large overcurrent and short-circuit faults. The turn-off delay time is measured under different fault current levels ranging from 30A to 90A. The function of zener diode Z_1 in Fig. 5 is experimentally examined. The relationship between turn-off delay time and fault current level is depicted in Fig. 10. As seen, protection circuit with Z_1 manages to turn off the fault current I_D before the maximum allowable turn-off delay time. The threshold current I_{OC} of overcurrent protection is 32.5A, above which the turn-off delay time decreases from 60.85ms to 0.254ms when I_D is at 72.5A. The threshold current I_{SC} of short-circuit protection is 72.5A, above which

the allowable turn-off delay time becomes 75μs. The turn-off delay time exceeds the maximum limitation if zener diode Z_1 is not used.

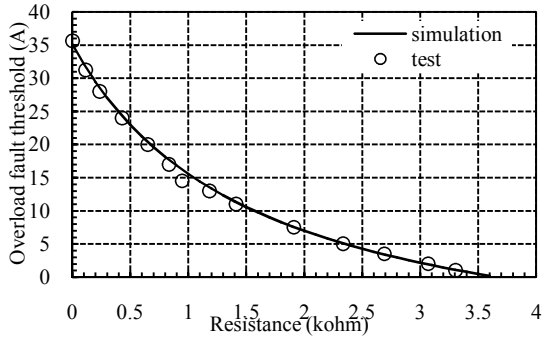

Figure 8. The relationship between overload fault current threshold I_{LD} and resistance R_4

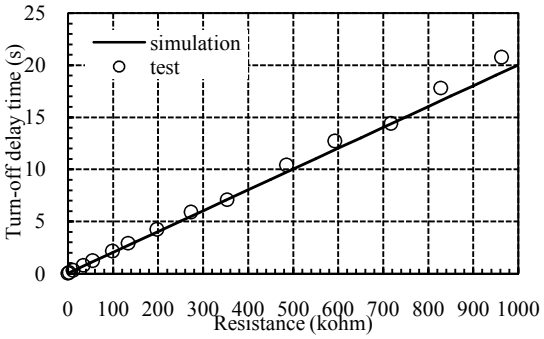

Figure 9. The relationship between overload turn-off delay time t_{LD} and resistance R_{11}

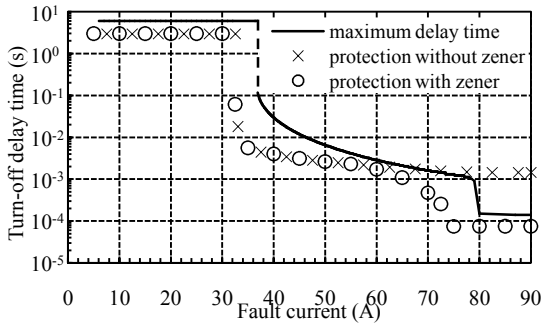

Figure 10. Turn-off delay time of tested circuit under different fault current level

V. CONCLUSIONS

This paper describes a variable time-delay overcurrent protection scheme for SiC MOSFET circuit breakers used in DC microgrid. The proposed scheme provides comprehensive protection for all overcurrent conditions with a proper current-dependent turn-off delay time. The proposed scheme is verified through laboratory measurements and the effectiveness of protection scheme is clearly confirmed.

ACKNOWLEDGMENT

This research is funded by the Republic of Singapore's National Research Foundation through a grant to the Berkeley Education Alliance for Research in Singapore (BEARS) for the Singapore-Berkeley Building Efficiency and Sustainability in the Tropics (SinBerBEST) Program. BEARS has been established by the University of California, Berkeley as a center for intellectual excellence in research and education in Singapore

REFERENCES

[1] C. Meyer, M. Kowal, and R. W. De Doncer, "Circuit breaker concepts for future high-power DC-applications," in *40th Industry Applications Annu. Meeting*., Hong Kong, 2005, pp. 860-866.

[2] M. Richard and M. Peter, "Comparison of advantages and disadvantages of electronic and mechanical protection systems for higher voltage DC 400V," in *Proc. 2013 Telecommunications Energy Conf.*, Hamburg, 2013, pp. 236-242.

[3] B. W. Williams, "The power MOSFET," in *Principles and Elements of Power Electronics*, Glasgow, England: Strathclyde Univ, 2006, ch. 4, pp. 116-117.

[4] S. Anand and B. G. Fernandes, "Optimal voltage level for DC microgrids," in *36th Ann. Conf. Industrial Electronics Society*, Glendale, AZ , 2010, pp. 3034 – 3039.

[5] R. J. Callanan, A. Agarwal, and A. Burk, *et al*., "Recent progress in SiC DMOSFETs and JBS Diodes at Cree," in *36th Ann. Conf. Industrial Electronics*, Orlando, FL, 2008, pp. 2885-2890.

[6] D. Dibra, M. Stecher, and S. Decker, *et al*., "On the origin of thermal runaway in a trench power MOSFET," in *IEEE Trans. Electron Devices*, vol. 58, no. 12, pp. 3477-3483, Oct. 2011.

[7] H. Medjahead, P. E. Vidal, and B. Nogarede, "Comparison between electromagnetic and thermal stress induced by direct current flow in IGBT bond wires," in *7th Int. Conf. Integrated Power Electronics Systems*, Nuremberg, 2012, pp. 1-6.

[8] X. Feng and A. V. Radun, "SiC based solid state power controller," in *23th Annu. Applied Power Electronics Conf. and Expo*., Austin, TX, 2008, pp. 1855-1860.

[9] K. Sakamoto, N. Fuchigami, H. Tsunoda, and E. Yanokura, "A fast-switching intelligent power MOSFET with thermal protection and negative gate protection," in *Int. Symp. Power Semiconductor Devices and IC's*, Weimar, 1997, pp. 189-192.

[10] U. Drofenik and J. W. Kolar, "A thermal model of a forced-cooled heat sink for transient temperature calculations employing a circuit simulator," in *IEEE Trans. Industry Applications*, vol. 126, no. 7, pp. 841-851, 2006.

[11] *Motors and Generators*, NEMA Standard MG 1-1998. Rev. 3, 2002.

[12] D. Salomonsson, L. Soder, and A. Sannino, "Protection of Low-Voltage DC Microgrids," in *IEEE Trans. Power Delivery*, vol. 24, no. 3, pp. 1045-1053, Jul. 2009.

[13] *CMF2010D-Silicon Carbide Power MOSFET*, Rev. D, CREE Inc., Durham, NC, 2012.

[14] J. Luo, Y. C. Liang, and B. J. Cho, "Design of LIGBT protection circuit for smart power integration," in *IEEE Trans. Industrial Electronics*, vol. 47, no. 4, pp. 744-750, Aug. 2000.

[15] K. Sheng, "Maximum junction temperatures of SiC power devices," in *IEEE Trans. Electron Devices*, vol. 52, no. 2, pp. 337-342, Feb. 2009.

[16] *Providing continuous gate drive using a charge pump*, TI Co., Dellas, TX, 2011, pp. 4-6.